

ERS-SAR Images a Bridge

J. Robalo¹ & J. Lichtenegger²

¹ESA-ESRIN national trainee

Instituto Hidrográfico, Rua das Trinas 49, 1249-093 Lisboa, Portugal

²ESA Directorate of Application Programmes, Earth Observation Applications Department
ESA-ESRIN, Via Galileo Galilei, 00044 Frascati, Italy

SAR imaging results are sometimes very peculiar, especially in the case of bridges. In particular, suspension bridges show complex radar signatures allowing the extraction of information concerning their shape and height. This article focuses on one such example, the '25 de Abril' bridge at the Tejo estuary close to Lisbon, Portugal (Fig. 1).

Introduction

Among the factors influencing the radar signature of a bridge are the spatial resolution of the observing system, the bridge architecture and its building materials. Suspension bridges, in particular, are generally high, and often constructed in steel. They are likely to produce bright, well-defined and sometimes complex SAR signatures. Pillar-supported metal bridges may in some way be assimilated to a suspension bridge, however, if they are covered with concrete and used as a roadway, they appear dark. In this case, the only mechanism that can provide a strong level of backscatter is the corner reflection (Fig. 2, path 2).

The image of a bridge also depends on its orientation relative to the flight track of the sensing platform. Bridges oriented in range direction appear as a single feature, independent of their structure type. Imaged in all other orientations, the representation of the bridge can be composed of various elements resulting from reflections of the water surface and of bridge sections (Fig. 2).

The environmental conditions of the surroundings of the bridge have also to be considered, especially in the case of a bridge over a body of water. Normally, strong corner reflection occurs. However, this effect might be weak or even absent due to the roughening of the surface by wind.

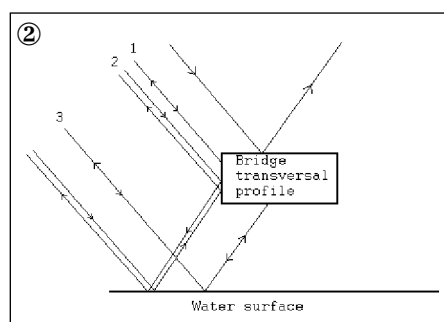


View of the '25 de Abril' bridge, with Lisbon in the background

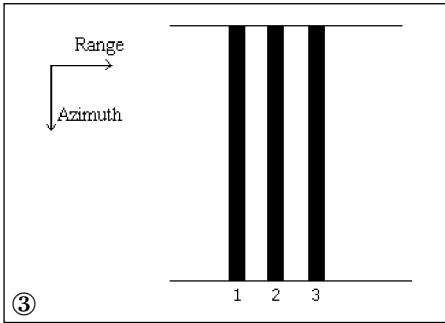
Suspension Bridges

An initial consideration when analysing radar targets concerns the characteristics of the image. In this case

The three paths of the backscattered signals



ERS-SAR PRI, which means ground range images were used. With regard to the viewable features (Fig.3), the following can be deduced: the shortest slant range is associated with the direct reflection from the bridge (Fig. 2, path 1) and is represented by the stripe closest to the satellite track. The corner-reflector effect (Fig. 2, path 2) is responsible for a second stripe. Reflections from under the bridge (Fig. 2, path 3) produce a third stripe. The three stripes are evenly separated in the radar image, and the distance in between is linked to the height of the bridge. Considering that the spatial resolution of an ERS-SAR PRI is 25m, for a low bridge the three stripes will merge into one.



Radar signature of a suspension steel bridge

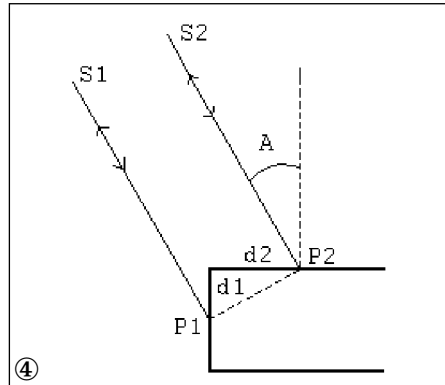
In reality, the process of formation of a radar signature from a bridge is much more complex. Many different points of the bridge have the same slant range (Figs. 4, 5 & 6) and electromagnetic waves also experience multiple reflections on the structure of the bridge. However, the overall effect is just the enhancement and broadening of the stripes.

The real position of the bridge is represented by stripe no. 2 (Fig. 3). This conclusion is based on the analysis of the imaging mechanism of the bridge's pillar stands, which mark the position of the bridge. In Figure 7, S2 represents the slant range of a radar pulse affected by corner reflection near the base of the stand. For practical purposes, the path of the pulse between the two reflecting surfaces (water and concrete wall) is neglected. S1 is the slant range associated with stripe no. 2. The comparison of S1 and S2 shows that they have the same value.

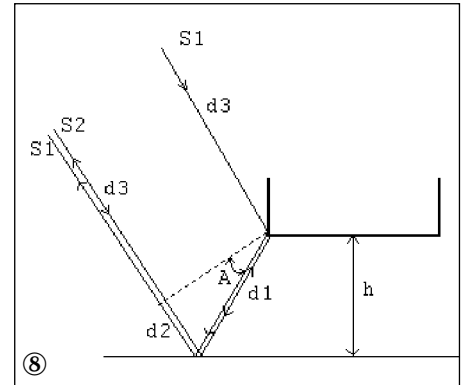
Height of a Bridge

As for the bridge height, a simple geometrical analysis of the slant ranges associated with stripes 2 and 3 provides a formula for calculation. From Figure 8, assuming A as the incidence angle, the following relations can be deduced:

$$\left. \begin{aligned} S2 - S1 &= \frac{d1 + d2}{2} \\ h &= \frac{d1 + d2}{2 * \cos(A)} \end{aligned} \right\} \Rightarrow h = \frac{S2 - S1}{\cos(A)}$$



Direct reflection: points P1 and P2 have the same slant range



Bridge height calculation

The slant range cannot be measured directly in a PRI image, since it is delivered in ground range. However, the ground range difference can be converted into slant range difference. Assuming a flat Earth and approximating spherical waves by plan waves, the relation between ground and slant range differences is given by:

$$S2 - S1 = (G2 - G1) * \sin(A)$$

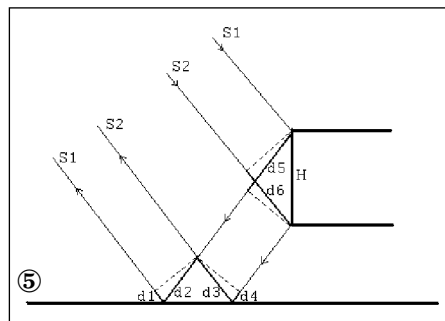
This leads to the formula:

$$h = (G2 - G1) * \tan(A)$$

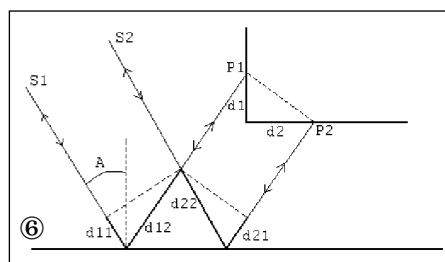
where G2-G1 is the ground range difference between the two features, in our case the distance between stripes 1 and 2 (Fig. 3), measured in the PRI image.

The "25 de Abril" Bridge

Figure 9 shows the Tejo estuary with the '25 de Abril' bridge at the harbour

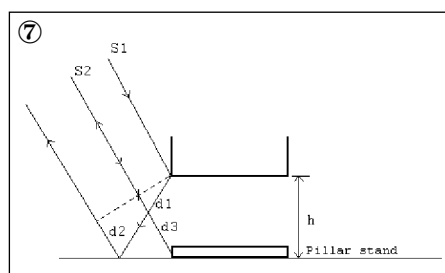


Corner reflection: every point along section H has the same slant range

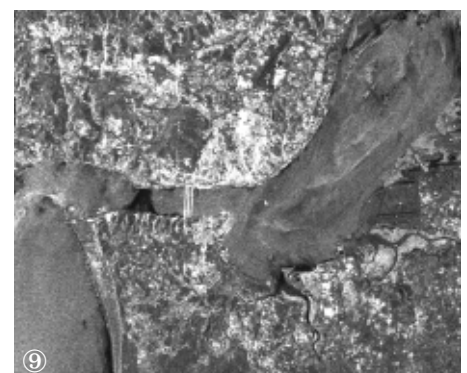


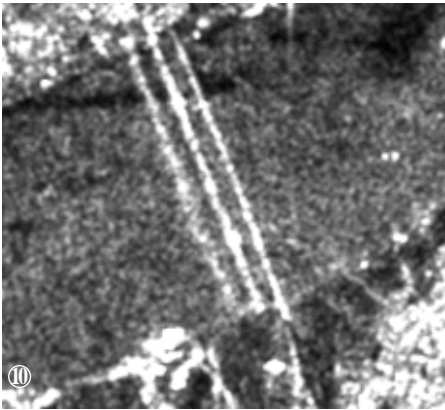
Multiple reflection: points P1 and P2 have the same slant range

Estimation of the real position of the bridge

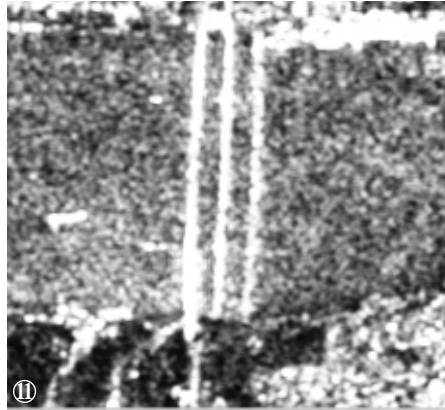


ERS-SAR PRI image of the Tejo estuary, 23 August 1998

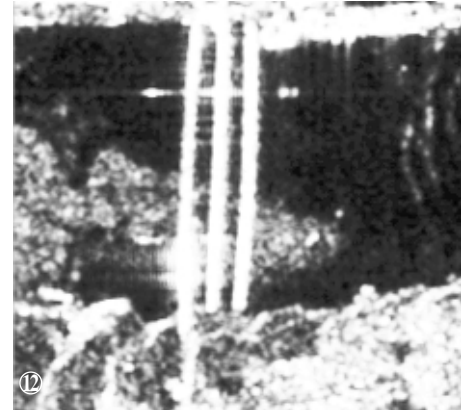




ERS-SAR PRI image of bridge '25 de Abril', 2 June 1992 (descending pass): the stripe to the right corresponds to directly backscattered signals



ERS-SAR PRI image of bridge '25 de Abril', 14 June 1998 (ascending pass): the stripe to the left corresponds to directly backscattered signals



ERS-SAR PRI image of bridge '25 de Abril', 5 April 1998 (ascending pass)

entrance, marked by three very distinct bright stripes. The 'Vasco da Gama' bridge, to the right, is only faintly visible. Judging from several data sets analysed, the main factors affecting the imaging of the '25 de Abril' bridge are the direction of the satellite passes and the wind speed.

A comparison of Figure 10 (descending pass) and Figure 11 (ascending pass) shows that the stripe located the farthest from the satellite flight track is dimmed when compared with the other two. This is the evidence of a weaker return signal, associated with a multiple reflection path, with power losses along the way. Moreover, wind can produce scattering Bragg-scale waves and the sea-state conditions will be less favourable for specular reflections, influencing paths 2 and 3 (Fig. 2) in Figures 10 and 11.

The effect of low wind is shown very clearly in Figure 12: the stripes are

brighter and the representation of the northern pillar is quite good. This pillar generates a symmetrical image, due to the effects of the different types of reflections. Both point-like features correspond to the top of the pillar. Figure 14 probably explains why: there is a larger cap mounted at the top of the pillars and there is also a connecting horizontal joist at this point. To the left of the three stripes, the direct signal is visible and to the right, the water-reflected pillar top can be seen. From Figure 13, the pillar height can be expressed by the equation:

$$h = (G2 - G1) * \frac{\tan(A)}{2}$$

Note that in Figure 11 the direct backscattered signals from the top of both pillars are visible.

Height Calculations

For ERS-SAR, the incidence angle varies from about 19.5° at near range,

to about 26.5° at far range. Accurate calculations require a precise knowledge of the incidence angle for a specific pixel of a PRI scene. Using the method described in Laur et al. [1] and considering the central area of the bridge, the value of $\alpha_1 21.054^\circ$ is found. Table 1 shows the results of height calculations compared to the real dimensions.

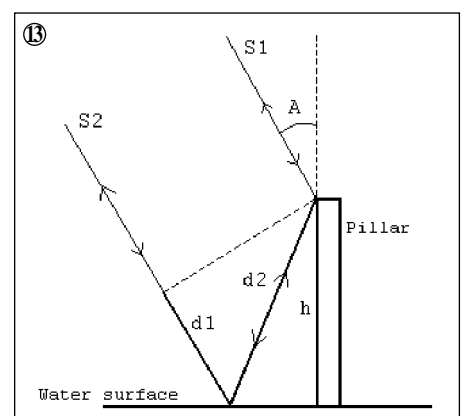
Conclusions

Suspension bridges have complex radar signatures. Once the interaction between the radar pulses and the bridge structure is clearly understood, ERS-SAR PRI images can provide information about the characteristics of this type of bridge. Generic formulas for

Table 1 Parameters and results for ERS-SAR image of 14 June 1998

	Bridge	Pillar
Incidence angle [°]	21.054	21.054
Ground range difference [m]	162	968
Calculated height [m]	62	186
Real height [m]	70	191

Pillar height calculation



the calculation of the bridge and pillar heights were determined. In our case the estimation of the height of the bridge was within 11% and the height of the pillar within 3% of the real values.

Acknowledgement

This paper reflects some results obtained in a study to get acquainted with radar remote sensing during a one-year trainee period granted by the Portuguese Government and ESA to the author¹. Later he concentrated his work opportunity on the use of ERS SAR for shallow-water bathymetry. He carried out an additional training at ARGOSS, in the Netherlands. His final report also included a study on the



feasibility to produce bathymetric maps in the Tejo estuary, jointly produced by the authors and ARGOSS.

References

- [1] Laur H., Bally P., Meadows P., Sanchez J., Schaettler B., and Lopinto E., "ERS SAR Calibration: Derivation of the backscattering coefficient σ^0 in ESA ERS SAR products", ESA Document No: ES-TN-RS-PM-HL09, Issue 2.2, 26 June 1996.
 - [2] Robalo J., "The imaging of bridges using ERS-SAR: Tejo estuary as a case study", ESA-ESRIN, September 1999.
 - [3] Sanchez, J. I., and Laur H., "The ERS SAR Products, Systems and Performances", *Proc. of the 3rd ERS Symposium*, Firenze, March 1997.
-